PHYSICAL REVIEW A VOLUME 45, NUMBER 7 1 APRIL 1992

Phase properties of fields generated in a multiphoton down-converter

R. Tanaś
Nonlinear Optics Division, Institute of Physics, Adam Mickiewicz University, 60-780 Poznań, Poland

Ts. Gantsog
Department of Theoretical Physics, Mongolian State University, Ulaanbaatar 210646, Mongolia

(Received 14 August 1991)

The phase properties of fields generated from the vacuum in the m-photon down-conversion process with quantum pumping are studied from the point of view of the Hermitian phase formalism. The joint phase distribution $P(\theta_a,\theta_b)$ as well as the marginal phase distribution $P(\theta_a)$ for the signal mode are derived and illustrated graphically for $m=2$, 3, and 4. The relationship between these phase distributions and the "classical" distributions obtained by integrating the Q function is established. It is shown that the classical phase distribution is a result of an averaging procedure that leads to a broadening of the phase distribution.

PACS number(s): 42.50.Dv

I. INTRODUCTION

A two-photon down-converter is known to produce optical fields with nonclassical properties [1–10]. It is essential for the quantum properties of fields generated in the process that the high-frequency pump photons be split into highly correlated pairs of lower-frequency signal and idler photons. In the simplest case of a nondepleted degenerate parametric process, the pump mode is assumed classical and nondepleted, and the signal and idler modes become one mode of the subharmonic field with half the frequency of the pump mode. In this case the time evolution of the subharmonic field can be found analytically and is described by a Bogoliubov transformation that maps the initial vacuum state into an ideal squeezed state [1–6]. The parametric down-conversion process turned out to be very effective in producing squeezed states in practice [11–16].

The states produced by the two-photon down-converter have interesting phase properties studied recently by Vaccaro and Pegg [17]; Schleich, Horowicz and Varro [18]; and Grønbech-Jensen, Christiansen, and Ramanujam [19] for the process with classical pumping and by Gantsog, Tanaś,and Zawodny [20] for the process with quantum pumping. The phase distribution of such states has two sharp peaks at the initial stages of the evolution that reflect the two-photon character of the process. If the quantum fluctuations of the pump mode are taken into account, the two peaks of the signal mode are broadened [20].

A generalization of the two-photon down-conversion to a multiphoton process has been initiated by Fisher, Nieto, and Sandberg [21] who have found that the vacuum-to-vacuum matrix elements of the evolution operators for such processes have divergent Taylor-series expansions in time, and they concluded that it must be something wrong with these evolution operators. Braunstein and McLachlan [22] have used the Padé summation technique that improved the convergence of series expansions, and they performed numerical calculations for the three- and four-photon processes showing the threefold and fourfold rotational symmetry of the Q-function contours. Elyutin and Klyshko [23] considered three-photon squeezing, showing that in the parametric approximation there are exploding solutions for such a process. The photon-number divergence in the multiphoton down-conversion has been discussed by Hillery [24], who has shown that the divergences are the result of the parametric approximation—that is, the assumption that the pump mode is classical and undepleted. If the pump mode is quantized and treated dynamically, the energy is conserved and there are no divergences in the multiphoton down-conversion. Recently, Braunstein and Caves [25] have discussed phase and homodyne statistics of such generalized squeezed states. They have calculated, in parametric approximation, the photocount distribution P_n, the Q function, and the classical phase distribution $P(\theta)$ for the states generated from the vacuum by the three- and four-photon down-converter. Their classical phase distribution, which is obtained by integrating $Q(\alpha)$ over the "radial" coordinate, shows the multipeak structure that corresponds to the rotational symmetry of the Q-function contours.

Gantsog, Tanaś, and Zawodny [20] have discussed the evolution of phase properties for the field generated by the two-photon down-converter with quantum pumping showing that quantum fluctuations of the pump mode lead to broadening of the phase distribution of the signal mode. To describe the phase properties of the field, they used the Hermitian phase formalism introduced by Pegg and Barnett [26–28]. This formalism allows calculations of the joint probability distribution $P(\theta_a,\theta_b)$ for the phases of the signal (θ_a) and pump (θ_b) modes, and once this function is known, all other phase characteristics can be found by taking integrals over θ_a and θ_b with the distribution $P(\theta_a,\theta_b)$. It has been shown that $P(\theta_a,\theta_b)$ evolves into a multipeak structure in the long-time limit, and in effect the phase distribution becomes more and more uniform, i.e., both phases randomized.

In this paper we study phase properties of the field generated in the multiphoton down-conversion process with quantum pumping. We employ the Hermitian phase formalism of Pegg and Barnett [26–28] to describe phase properties of the field. The joint phase probability distribution $P(\theta_a,\theta_b)$ as well as the marginal phase distribution $P(\theta_a)$ for the signal mode are obtained and illustrated graphically for the two-, three-, and four-photon processes. The multipeak structure that corresponds to the multiplicity of the process is revealed in the phase distributions. A comparison is made between the Pegg-Barnett phase distribution and the classical phase distribution obtained by integrating the $Q(\alpha)$ function over the amplitude. It is shown that the latter is broader than the former, and a general relation between the two is established. The phase distributions are compared to the corresponding Q-function pictures to visualize their symmetry properties for the multiphoton down-conversion processes. The quantum character of the pump mode is accounted for, and the exact quantum-mechanical evolution of the field state is obtained using the method of numerical diagonalization of the interaction Hamiltonian. For the pump mode being initially in a coherent state with a not-very-big mean number of photons, this method works very well, and all the field characteristics can be obtained in a direct and reliable way. This is particularly important for the three-and-more-photon processes for which there are no analytical solutions known, and there are some numerical problems in the parametric approximation.

II. QUANTUM EVOLUTION OF THE FIELD STATE

The m-photon down-conversion process with quantum pumping can be described by the following model Hamiltonian:

$$H=H_0+H_I=\hbar\omega a^\dagger a+m\hbar\omega b^\dagger b+\hbar g(b^\dagger a^m+ba^{\dagger m}) , \tag{1}$$

where $a(a^\dagger)$ and $b(b^\dagger)$ are the annihilation (creation) operators of the signal mode at frequency ω and the pump mode at frequency $m\omega$, respectively. The coupling constant g, which is real, describes the coupling between the two modes. The Hamiltonian (1) is identical for the m-photon down-conversion and the mth harmonic generation, and these are the initial conditions that distinguish between the two processes. In the case of harmonic generation, mode b is initially in the vacuum state and mode a is populated. For the down-conversion process considered in this paper, mode b (pump mode) is initially populated, while mode a (signal mode) is in the vacuum state. The distinction between the two processes is far from being trivial, and the states generated in the two processes have quite different properties.

Since H_0 and H_I commute, there are constants of motion: H_0 and H_I. H_0 determines the total energy stored in both modes, which is conserved by the interaction H_I. This enables us to factor out $\exp(-iH_0t/\hbar)$ from the evolution operator—in fact, to drop it altogether and to write the resulting state of the field as

$$|\psi(t)\rangle=\exp(-iH_It/\hbar)|\psi(0)\rangle , \tag{2}$$

where $|\psi(0)\rangle$ is the initial state of the field. Since the interaction Hamiltonian H_I is not diagonal in the number-state basis, to find the state evolution, we apply a numerical method to diagonalize H_I. Such method was used earlier for second-harmonic generation [29,30].

In this paper we consider the m-photon down-conversion process, which may be considered as a generalization of the parametric down-conversion process by accounting for the quantum properties of the pump mode. The Hamiltonian H_0, which is a constant of motion, implies the conservation of the quantity

$$\langle a^\dagger a\rangle+m\langle b^\dagger b\rangle=\text{const} , \tag{3}$$

and this prevents any exploding solutions. We assume the initial state of the field to be

$$|\psi(0)\rangle=\sum_{n=0}^{\infty} b_n|0,n\rangle , \tag{4}$$

where

$$b_n=\exp(-|\beta_0|^2)\frac{|\beta_0|^n}{\sqrt{n!}}e^{in\varphi_b} \tag{5}$$

is the Poissonian weight factor of the coherent state $|\beta_0\rangle$ of the pump mode with $\beta_0=|\beta_0|e^{i\varphi_b}$. The state $|0,n\rangle=|0\rangle|n\rangle$ is the product of the Fock states with n photons in the pump mode and no photons in the signal mode. That is, we assume the pump mode as being initially in a coherent state $|\beta_0\rangle$ and the signal mode as being initially in the vacuum. With these initial conditions the resulting state (2) can be written (in the interaction picture) as

$$|\psi(t)\rangle=\sum_{n=0}^{\infty} b_n\sum_{k=0}^{n} c_{mn,k}(t)|mk,n-k\rangle , \tag{6}$$

where the state $|mk,n-k\rangle$ is the state with $n-k$ photons in the pump mode and mk photons in the signal mode. The coefficients $c_{mn,k}(t)$ are the matrix elements of the evolution operator

$$c_{mn,k}(t)=\langle mk,n-k|\exp(-iH_It/\hbar)|0,n\rangle , \tag{7}$$

and they are calculated numerically by diagonalizing the interaction Hamiltonian. This allows us to find the evolution of the state (6).

III. PHASE PROPERTIES OF THE FIELD

To study the phase properties of the field generated in the m-photon down-conversion process, we employ the Pegg-Barnett [26–28] Hermitian phase formalism to find the joint phase distribution $P(\theta_a,\theta_b)$ as well as the marginal phase distribution $P(\theta_a)$ for the phase of the signal mode. The Pegg-Barnett formalism is based on introducing a finite $(s+1)$-dimensional space Ψ spanned by the number states $|0\rangle,|1\rangle,\ldots,|s\rangle$. The Hermitian phase operator operates on this finite space, and after all necessary expectation values have been calculated in Ψ, the value of s is allowed to tend to infinity. A complete orthonormal basis of $(s+1)$ phase states is defined on Ψ as

$$|\theta_m\rangle \equiv \frac{1}{\sqrt{s+1}} \sum_{n=0}^{s} \exp(in\theta_m)|n\rangle \ , \tag{8}$$

where

$$\theta_m \equiv \theta_0 + \frac{2\pi m}{s+1} \quad (m=0,1,\ldots,s) \ . \tag{9}$$

The value of θ_0 is arbitrary and defines a particular basis set of $(s+1)$ mutually orthogonal phase states. The Hermitian phase operator is defined as

$$\hat{\phi}_\theta \equiv \sum_{m=0}^{s} \theta_m |\theta_m\rangle\langle\theta_m| \ . \tag{10}$$

The phase states (8) are eigenstates of the phase operator (10) with the eigenvalues θ_m restricted to lie within a phase window between θ_0 and $\theta_0+2\pi$.

The expectation value of the phase operator (10) in a state $|\psi\rangle$ is given by

$$\langle\psi|\hat{\phi}_\theta|\psi\rangle = \sum_{m=0}^{s} \theta_m |\langle\theta_m|\psi\rangle|^2 \ , \tag{11}$$

where $|\langle\theta_m|\psi\rangle|^2$ gives the probability of being in the phase state $|\theta_m\rangle$. The density of phase states is $(s+1)/2\pi$, so in the continuum limit, as s tends to infinity, we can write Eq. (11) as

$$\langle\psi|\hat{\phi}_\theta|\psi\rangle = \int_{\theta_0}^{\theta_0+2\pi} \theta P(\theta) d\theta \ , \tag{12}$$

where the continuum phase distribution $P(\theta)$ is introduced by

$$P(\theta) = \lim_{s\to\infty} \frac{s+1}{2\pi} |\langle\theta_m|\psi\rangle|^2 \ , \tag{13}$$

where θ_m has been replaced by the continuous phase variable θ. Once the phase distribution function $P(\theta)$ is known, all the quantum-mechanical phase expectation values can be calculated with this function in a classical-like manner by integrating over θ. The choice of θ_0 defines the particular window of phase values.

In our case of a field produced in the m-photon down-conversion process with quantum pumping, the state of the field (6) is in fact a two-mode state, and the phase formalism must be generalized to the two-mode case. The generalization is straightforward and obvious, and for the state (6) we obtain

$$\langle\theta_{m_a}|\langle\theta_{m_b}|\psi(t)\rangle = (s_a+1)^{-1/2}(s_b+1)^{-1/2} \sum_{n=0}^{s_a} b_n \sum_{n=0}^{n} \exp\{-i[mk\theta_{m_a} + (n-k)\theta_{m_b}]\} c_{mn,k}(t) \ . \tag{14}$$

We use the indices a and b to distinguish between the signal (a) and pump (b) modes. There is still a freedom of choice in (14) of the values of $\theta_0^{a,b}$, which define the phase window. We can choose these values at will, so we take them as

$$\theta_0^{a,b} = \varphi_{a,b} - \frac{\pi s_{a,b}}{s_{a,b}+1} \ , \tag{15}$$

and we introduce the new phase values

$$\theta_{\mu_{a,b}} = \theta_{m_{a,b}} - \varphi_{a,b} \ , \tag{16}$$

where the new phase labels $\mu_{a,b}$ run between the values $-s_{a,b}/2$ and $s_{a,b}/2$ with unit step. This means that we symmetrized the phase windows for the signal and pump modes with respect to the phases φ_a and φ_b, respectively.

On inserting (15) and (16) into (14), taking the modulus squared of (14), and taking the continuum limit by making the replacement

$$\sum_{\mu_{a,b}=-s_{a,b}/2}^{s_{a,b}/2} \frac{2\pi}{s_{a,b}+1} \to \int_{-\pi}^{\pi} d\theta_{a,b} \ , \tag{17}$$

we arrive at the continuous joint probability distribution for the continuous variables θ_a and θ_b, which has the form

$$P(\theta_a,\theta_b) = \frac{1}{(2\pi)^2} \left| \sum_{n=0}^{\infty} |b_n| \sum_{k=0}^{n} c_{mn,k}(t) \exp\{-i[mk\theta_a + (n-k)\theta_b + k(m\varphi_a - \varphi_b)]\} \right|^2 \ . \tag{18}$$

The distribution (18) is normalized so as

$$\int_{-\pi}^{\pi}\int_{-\pi}^{\pi} P(\theta_a,\theta_b) d\theta_a d\theta_b = 1 \ . \tag{19}$$

To fix the phase windows for θ_a and θ_b, we have to assign to φ_a and φ_b particular values. It is interesting to note that formula (18) depends on the phase difference $m\varphi_a - \varphi_b$ only. This reproduces the classical phase relation for the parametric amplifier, and classically this quantity should be equal to $-\pi/2$ to get the amplification of the signal mode (if the coupling constant g is positive). Such a choice means that a peak should appear in the phase distribution at $\theta_a=0$. As will become clear later, the phase distribution for the m-photon down-conversion exhibits an m-peak structure along the θ_a direction, and the choice of the phase window that minimizes the phase variance is $m\varphi_a - \varphi_b = \pi/2$ for m even and $m\varphi_a - \varphi_b = -\pi/2$ for m odd. We choose the phase window following this rule.

The phase distribution $P(\theta_a,\theta_b)$ is shown in Fig. 1 for $m=2$, 3, and 4. The m-peak structure of the joint phase distribution is quite evident, and it reflects the mathematical property of the function $P(\theta_a,\theta_b)$ which shows periodicity in θ_a with period $2\pi/m$. From the point of view of the pump mode, we see only one peak at $\theta_b=0$, which represents the phase of the initially coherent state of the pump mode. For numerical reasons we use the mean number of photons N_b in the pump mode rather small, but for $N_b>1$ the multipeak structure of the distribution is well resolved. For larger N_b the phase peaks become sharper. The symmetry inherent in this phase distribution is the same as obtained earlier by Braunstein and Caves [25] for the generalized squeezed states from their study of the Q function and the classical phase distribution of the signal mode. To make the comparison of both approaches more evident, we calculate the Q function as well as the classical phase distribution for our case of the down-converter with quantum pumping.

For the two-mode field considered in this paper, we can calculate the two-mode Q function as

$$\begin{aligned} Q(\alpha,\beta) = |\langle \alpha,\beta|\psi(t)\rangle|^2 &= \left| \sum_{n=0}^{\infty} b_n \sum_{k=0}^{n} c_{mn,k}(t) \langle \alpha | mk \rangle \langle \beta | n-k \rangle \right|^2 \\ &= \left| \sum_{n=0}^{\infty} b_n \sum_{k=0}^{n} c_{mn,k}(t) \exp(-|\alpha|^2/2) \frac{|\alpha|^{mk}}{\sqrt{(mk)!}} e^{-imk\theta_a} \exp(-|\beta|^2/2) \frac{|\beta|^{n-k}}{\sqrt{(n-k)!}} e^{-i(n-k)\theta_b} \right|^2 , \end{aligned} \tag{20}$$

where we have assumed

$$\alpha = |\alpha| e^{i\theta_a}, \quad \beta = |\beta| e^{i\theta_b} . \tag{21}$$

Comparing Eqs. (20) and (18), one can easily check that the phase dependence of $Q(\alpha,\beta)$ is exactly the same as in $P(\theta_a,\theta_b)$, when we identify the phases of α and β as in Eq. (21) and introduce the reference phases φ_a and φ_b as in Eq. (18). Performing the integrations over the amplitudes $|\alpha|$ and $|\beta|$ in Eq. (20), we arrive at the "classical" two-mode phase distribution $P_{\text{class}}(\theta_a,\theta_b)$. The term "classical" is used here in the sense used by Braunstein and Caves [25], who refer to such a phase measurement as effectively classical, since the Q function applies to simultaneous measurement of two noncommuting observables, a process that inevitably introduces additional noise. After integrating, we have

$$\begin{aligned} P_{\text{class}}(\theta_a,\theta_b) &= \frac{1}{\pi^2} \int_0^{\infty} \int_0^{\infty} Q(\alpha,\beta) |\alpha| |\beta| d|\alpha| d|\beta| \\ &= \frac{1}{(2\pi)^2} \sum_{n,n'=0}^{\infty} |b_n| |b_{n'}| \sum_{k=0}^{n} \sum_{k'=0}^{n'} c_{mn,k}(t) c^*_{mn',k'}(t) \\ &\qquad \times \exp\{-i[m(k-k')\theta_a + (n-k-n'+k')\theta_b + (k-k')(m\varphi_a - \varphi_b)]\} \\ &\qquad \times F(mk,mk') F(n-k,n'-k') , \end{aligned} \tag{22}$$

where the reference phases φ_a and φ_b have been introduced explicitly to be in agreement with Eq. (18), and we have obtained the extra factors

$$F(n,k) = \frac{\Gamma((n+k)/2+1)}{\sqrt{n!k!}} . \tag{23}$$

It is evident from Eq. (22) that these are the extra factors $F(mk,mk')$ and $F(n-k,n'-k')$ that distinguish the classical phase distribution (22) from the Pegg-Barnett phase distribution (18). Our derivation of formula (22) is quite general so we expect it to be applicable to any state of the field with known number-state decomposition.

It is difficult to illustrate the two-mode Q function given by formula (20), since it is a function of four real variables. It we are interested in the properties of the signal mode, however, we can define the Q function for this mode by

$$\begin{aligned} Q(\alpha) = \frac{1}{\pi} \int Q(\alpha,\beta) d^2\beta &= \sum_{n=0}^{\infty} |b_n|^2 \sum_{k=0}^{n} |c_{mn,k}(t)|^2 |\langle \alpha | mk \rangle|^2 \\ &\quad + 2\,\mathrm{Re} \left[\sum_{n>n'}^{\infty} b_n b^*_{n'} \sum_{k=0}^{n} \sum_{k'=0}^{n'} c_{mn,k}(t) c^*_{mn',k'}(t) \langle \alpha | mk \rangle \langle \alpha | mk' \rangle^* \delta_{n-n',k-k'} \right] , \end{aligned} \tag{24}$$

where

$$\langle \alpha | mk \rangle = \exp(-|\alpha|^2/2) \frac{|\alpha|^{mk}}{\sqrt{(mk)!}} e^{-imk\theta_a} . \tag{25}$$

This function [Eq. (24)] is illustrated graphically in Fig. 2 for $m=2$, 3, and 4. The other parameters are taken the same as those for the phase distributions shown in Fig. 1. The m-fold rotational symmetry of the $Q(\alpha)$ that corresponds to the m-peak structure of the phase distribution is clearly visible, and it is similar to the results obtained in the parametric approximation [22,25]. The contour plots of $Q(\alpha)$ shown in Fig. 3 make the similarity of our results to those of Braunstein and Caves [25] even more convincing, although we take different values of the evolution time. To illustrate the symmetry of the distributions, we have chosen the times at the early stages of the evolution when the joint phase distribution has a clear m-peak structure. It has been shown that for later times, in the case of both the two-photon down-conversion with quantum pumping [20] and the second-harmonic generation [31,32], the phase distribution goes through a sequence of bifurcations towards a multipeak structure with more and more uniform phase distribution.

Integrating the joint phase distribution $P(\theta_a,\theta_b)$, or $P_{\text{class}}(\theta_a,\theta_b)$, over θ_b, we get the marginal phase distribution $P(\theta_a)$, or $P_{\text{class}}(\theta_a)$, of the signal mode phase θ_a. We concentrate on the marginal phase distribution for the signal mode to show explicitly the difference between the Pegg-Barnett phase distribution $P(\theta_a)$ and the "classical" phase distribution $P_{\text{class}}(\theta_a)$. For $P_{\text{class}}(\theta_a)$ we have

$$\begin{aligned} P_{\text{class}}(\theta_a) &= \int_{-\pi}^{\pi} P_{\text{class}}(\theta_a,\theta_b)\,d\theta_b \\ &= \frac{1}{\pi}\int_0^{\infty} Q(\alpha)|\alpha|\,d|\alpha| \\ &= \frac{1}{2\pi}\left[1+2\,\mathrm{Re}\sum_{n>n'} |b_n|\,|b_{n'}| \sum_{k=0}^{n}\sum_{k'=0}^{n'} c_{mn,k}c^{*}_{mn',k'}\exp[-i(k-k')(m\theta_a+m\varphi_a-\varphi_b)]\delta_{n-n',k-k'}F(mk,mk')\right], \end{aligned} \tag{26}$$

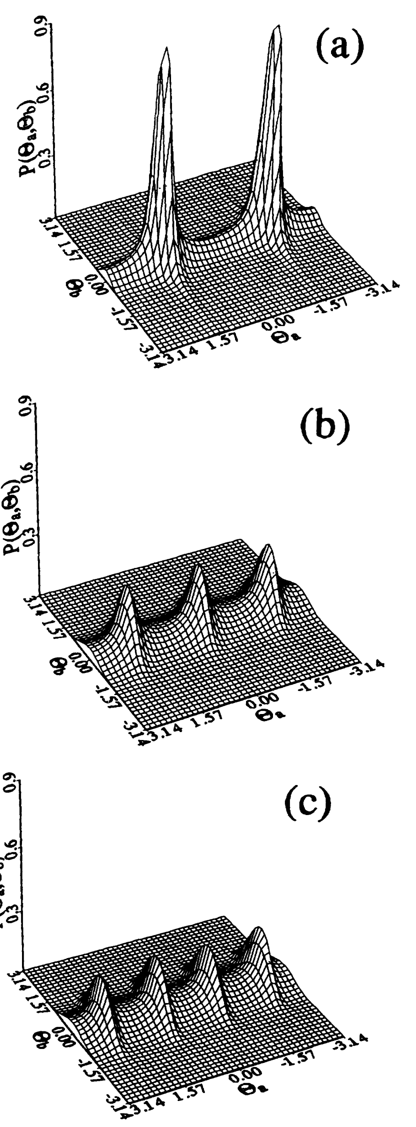

FIG. 1 Plots of the joint phase distribution $P(\theta_a,\theta_b)$ for the states generated in the m-photon down-conversion: (a) $m=2$, $N_b=4$, $gt=0.3$; (b) $m=3$, $N_b=2$, $gt=0.025$; (c) $m=4$, $N_b=2$, $gt=0.005$.

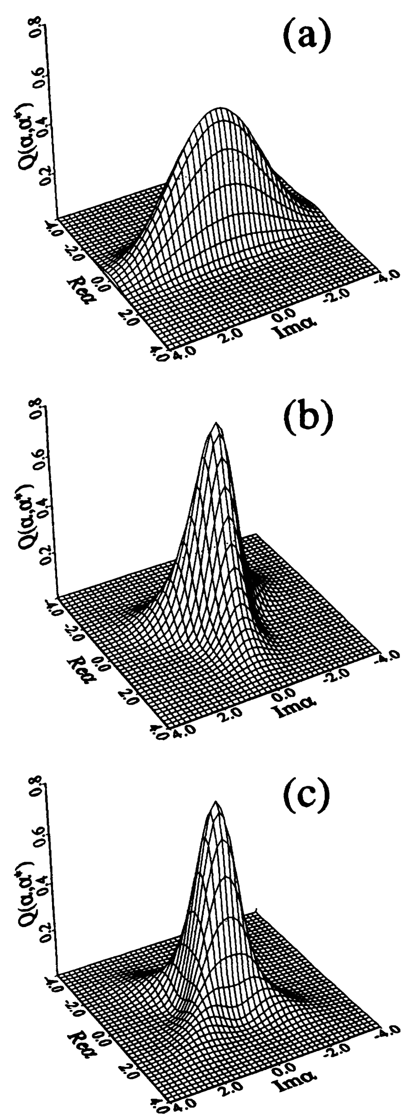

FIG. 2 Three-dimensional plots of the Q function $Q(\alpha)$ for the signal mode. The parameters are the same as in Fig. 1.

where we have introduced the reference phases φ_a and φ_b to have the same phase window as we used for the Pegg-Barnett phase distribution; b_n are given by Eq. (5). It is easy to check that the Pegg-Barnett phase distribution $P(\theta_a)$, which is defined as

$$P(\theta_a)=\int_{-\pi}^{\pi} P(\theta_a,\theta_b)d\theta_b \ , \tag{27}$$

with $P(\theta_a,\theta_b)$ given by Eq. (18), can be equivalently obtained from formula (26) by putting $F(mk,mk')=1$. Thus, as in the joint phase probability, the difference between the Pegg-Barnett and the classical results consists in the presence of additional factors $F(mk,mk')$ defined by Eq. (23) in $P_{\text{class}}(\theta_a)$. The polar coordinate plots of the two functions are shown in Fig. 4, for $m = 2$, 3, and 4. The difference between the two is quite evident. The classical phase distribution is broader than the Pegg-Barnett distribution, although the rotational symmetry, i.e., the peak structure, is the same. The broadening of the classical phase distribution with respect to the quantum Pegg-Barnett distribution makes the use of the word "classical" more understandable. This broadening is a result of diminishing of the nondiagonal elements that define the phase structure by the factor $F(mk,mk')$. The elements $F(n,k)$ defined by Eq. (23) are symmetrical, $F(n,k)=F(k,n)$; their diagonal elements are unity,

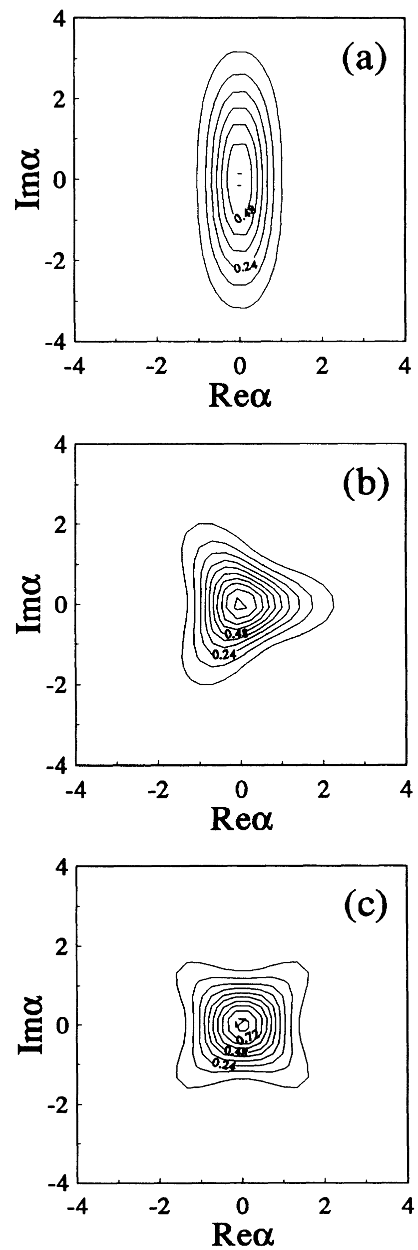

FIG. 3. Contour plots of the Q function $Q(\alpha)$ for the signal mode. The parameters are the same as in Fig. 1.

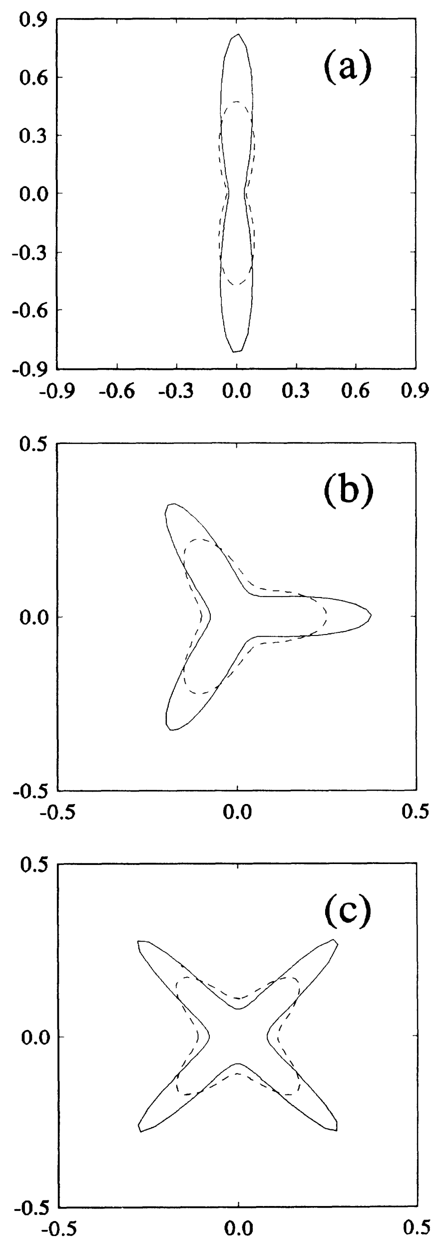

FIG. 4. The polar-coordinate plots of the marginal phase distribution for the signal mode: the Pegg-Barnett distribution $P(\theta_a)$ (solid line) and the "classical" phase distribution $P_{\text{class}}(\theta_a)$ (dashed line). The parameters are the same as in Fig. 1.

$F(n,n)=1$; and they can be easily calculated with the following recurrence formula:

$$F(n+1,k)=\frac{F(n,k)}{\sqrt{n+1}}\begin{cases}\left[\dfrac{n+k}{2}+1\right]\sqrt{\pi}\displaystyle\prod_{s=1}^{s_m}[1-(1/2s)] & \text{for } n+k \text{ even}\\ \left[\sqrt{\pi}\displaystyle\prod_{s=1}^{s_m}[1-(1/2s)]\right]^{-1} & \text{for } n+k \text{ odd ,}\end{cases} \tag{28}$$

where

$$s_m=n+k+1-\left[\frac{n+k+1}{2}\right], \tag{29}$$

and $[\cdots]$ in Eq. (29) means the integer part of the bracketed number. The behavior of the coefficients $F(n,k)$ is illustrated in Fig. 5. The farther away we go from the diagonal $F(n,n)=1$, the smaller are $F(n,k)$, although the rate of decay decreases as the numbers n,k increase. Knowing the coefficients $F(n,k)$, we can directly get the classical phase distribution from the Pegg-Barnett distribution by weighting the nondiagonal phase elements with their "probabilities" $F(n,k)$. This procedure can be considered as an averaging of the Pegg-Barnett phase distribution. Looking at Figs. 4 and 5, we may conclude that the averaged phase distributions plotted in polar coordinates are quite similar to the contour plots of the Q function. The Pegg-Barnett phase distribution gives the pictures with much better formed lobes, i.e., with much sharper phase peaks.

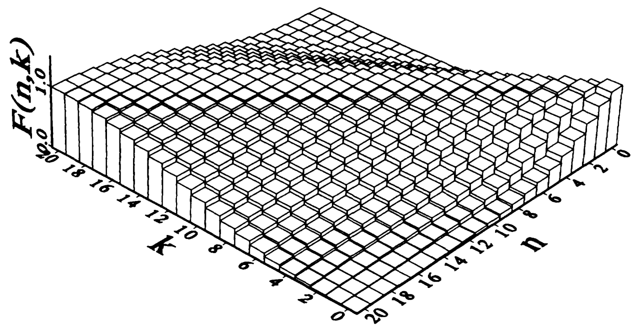

FIG. 5. Distribution of the coefficients $F(n,k)$.

IV. CONCLUSION

We have discussed phase properties of the fields produced by the m-photon down-converter with quantum pumping. We have derived the joint phase distribution $P(\theta_a,\theta_b)$ as well as the marginal phase distribution $P(\theta_a)$ for the signal mode using the Pegg-Barnett phase formalism. These two phase distributions are compared to the classical phase distributions $P_{\text{class}}(\theta_a,\theta_b)$ and $P_{\text{class}}(\theta_a)$ obtained by integrating the Q functions. It is shown that there is a universal relationship between the classical phase distributions and the Pegg-Barnett phase distributions. The former are obtained from the latter by an averaging procedure. This procedure is defined in the paper.

To find the state evolution, we have used the method of numerical diagonalization of the interaction Hamiltonian, which allows us to find the matrix elements of the evolution operator and, consequently, the state evolution. All the formulas can be expressed in terms of the coefficients $c_{mn,k}(t)$ being the matrix elements of the evolution operator. Our calculations are performed for an initially coherent state of the pump mode, so we can compare our results to the results obtained, in the parametric approximation (classical and nondepleted pumping), by Braunstein and Caves [25]. For numerical reasons the mean numbers of photons of the pump mode we take in our calculations are rather small. However, for $N_b>1$, we obtain the results very similar to those of Braunstein and Caves [25]. In contrast to the parametric approximation, the fully quantum approach allows the avoidance of some divergences that appear in the parametric approximation [23,24].

The phase distributions for the field produced in the m-photon down-conversion process exhibit the m-fold symmetry, which is best visualized when the marginal phase distribution $P(\theta_a)$ is plotted in polar coordinates. We have shown that the "classical" phase distribution obtained by integrating the Q function is broader than the Pegg-Barnett phase distribution, although in the case of the m-photon down-conversion, its symmetry, or the peak structure, is the same.

The m-fold symmetry of the phase distributions appears in its most striking form at the initial stages of the evolution. The quantum fluctuations of the pump mode lead to spreading out the phase distribution at later stages. It has been shown for the two-photon down-conversion [20] and the second-harmonic generation [31,32] that the phase distribution changes its character when the first maximum of the generated mode has been reached. This is associated with the transition from the down-conversion to the second-harmonic generation regime (or vice versa). So there is a limit, imposed by the quantum pumping, on the applicability of the parametric approximation.

[1] H. Takahasi, Adv. Commun. Syst. **1**, 227 (1965).
[2] D. Stoler, Phys. Rev. D **1**, 3217 (1970); **4**, 1925 (1971).
[3] E. Y. C. Lu, Nuovo Cimento Lett. **2**, 1241 (1971).
[4] H. P. Yuen, Phys. Rev. A **13**, 2226 (1976).
[5] J. N. Hollenhorst, Phys. Rev. D **19**, 1669 (1979).
[6] C. M. Caves, Phys. Rev. D **23**, 1693 (1981).
[7] S. Friberg, C. K. Hong, and L. Mandel, Phys. Rev. Lett **54**, 2011 (1985).
[8] M. D. Reid and D. F. Walls, Phys. Rev. A **34**, 1260 (1986).
[9] Z. Y. Ou and L. Mandel, Phys. Rev. Lett. **61**, 50 (1988).
[10] S. M. Tan and D. F. Walls, Opt. Commun. **71**, 235 (1989).
[11] L. A. Wu, H. J. Kimble, J. L. Hall, and H. Wu, Phys. Rev. Lett. **57**, 2520 (1986).
[12] A. Heidmann, R. Horowicz, S. Reynaud, E. Giacobino, C.

Fabre, and G. Camy, Phys. Rev. Lett. **59**, 2555 (1987).
[13] R. Slusher, P. Grangier, A. LaPorta, B. Yurke, and M. Potasek, Phys. Rev. Lett. **59**, 2566 (1987).
[14] S. Pereira, M. Xiao, H. J. Kimble, and J. Hall, Phys. Rev. A **38**, 4931 (1988).
[15] P. R. Tapster, J. G. Rarity, and J. S. Satchell, Phys. Rev. A **37**, 2963 (1988).
[16] T. Debuischert, S. Reynaud, A. Heidmann, E. Giacobino, and C. Fabre, Quantum Opt. **1**, 3 (1989).
[17] J. A. Vaccaro and D. T. Pegg, Opt. Cummun. **70**, 529 (1989).
[18] W. Schleich, R. J. Horowicz, and S. Varro, Phys. Rev. A **40**, 7405 (1989).
[19] N. Grønbech-Jensen, P. L. Christiansen, and P. S. Ramanujam, J. Opt. Soc. Am. B **6**, 2423 (1989).
[20] Ts. Gantsog, R. Tanaś, and R. Zawodny, Opt. Commun. **82**, 345 (1991).
[21] R. A. Fisher, M. M. Nieto, and V. D. Sandberg, Phys. Rev. D **29**, 1107 (1984).
[22] S. L. Braunstein and R. L. McLachlan, Phys. Rev. A **35**, 1659 (1987).
[23] P. V. Elyutin and D. N. Klyshko, Phys. Lett. **149A**, 241 (1990).
[24] M. Hillery, Phys. Rev. A **42**, 498 (1990).
[25] S. L. Braunstein and C. M. Caves, Phys. Rev. A **42**, 4115 (1990).
[26] D. T. Pegg and S. M. Barnett, Europhys. Lett. **6**, 483 (1988).
[27] S. M. Barnett and D. T. Pegg, J. Mod. Opt. **36**, 7 (1989).
[28] D. T. Pegg and S. M. Barnett, Phys. Rev. A **39**, 1665 (1989).
[29] D. F. Walls and C. T. Tindle, Nuovo Cimento Lett. **2**, 915 (1971); J. Phys. A **8**, 534 (1972).
[30] J. Mostowski and K. Rzążewski, Phys. Lett. **66A**, 275 (1978).
[31] Ts. Gantsog, R. Tanaś, and R. Zawodny, Phys. Lett **155A**, 1 (1991).
[32] R. Tanaś, Ts. Gantsog, and R. Zawodny, Quantum Opt. **3**, 221 (1991).